Journal of Asian Earth Sciences 35 (2009) 285–297

Contents lists available at ScienceDirect

Journal of Asian Earth Sciences

journal homepage: www.elsevier.com/locate/jaes

Two types of peridotite in North Qaidam UHPM belt and their tectonic implications for oceanic and continental subduction: A review

Shuguang Song [a,b,*], Li Su [b], Yaoling Niu [c], Guibin Zhang [a], Lifei Zhang [a]

[a] MOE Key Laboratory of Orogenic Belts and Crustal Evolution, School of Earth and Space Sciences, Peking University, Beijing 100871, China
[b] State Key Laboratory of Geological Processes and Mineral Resources, China University of Geosciences, Beijing 100083, China
[c] Department of Earth Science, Durham University, Durham DH1 3LE, UK

ARTICLE INFO

Article history:
Received 8 March 2008
Received in revised form 16 November 2008
Accepted 17 November 2008

Keywords:
Peridotite
Continental subduction and collision belt
Ultrahigh-pressure metamorphism
North Qaidam

ABSTRACT

Two types of peridotites are recognized in the North Qaidam *continental-type* UHP metamorphic belt. (1) Garnet peridotite, which includes garnet lherzolite, garnet-bearing dunite, garnet-free dunite and garnet pyroxenite, is one of the most informative lithologies in a *continental-type* subduction zone. Observations such as diamond inclusion in a zircon crystal and decompression exsolutions in garnet and olivine, plus thermobarometric calculations, argue that this garnet peridotite must have derived from mantle depths in excess of 200 km. Geochemical data reveal that the protolith of the garnet peridotite is largely of cumulate origin from high-Mg melts in a sub-arc mantle wedge environment rather than a abyssal peridotite. (2) Oceanic lithospheric mantle harzburgite, which occurs together with a meta-cumulate complex (including garnet pyroxenite and kyanite-eclogite) and with eclogite of MORB protolith. They are interpreted as exhumed blocks of the subducted oceanic lithosphere formed in the Cambrian (~500–550 Ma). The presence of these two types of peridotites in the same continental-type subduction belt is unique and they allow a better understanding of the tectonic history of the North Qaidam *continental-type* UHP belt in particular and processes of plate tectonic convergence from oceanic lithosphere subduction to continental collision/subduction in general.

1. Introduction

High-pressure metamorphic rocks within orogenic belts record dynamic Earth processes of subduction and exhumation of both oceanic and continental lithospheric materials. Paleo-subduction zones identified within continents may be conveniently divided into *oceanic-type* and *continental-type* in terms of lithological assemblages (Song et al., 2006), which are equivalent to the Pacific-type and Alpine-type (Ernst, 2001) or B-type and A-type (Maruyama et al., 1996) subduction zones in the literature. The general notion is that, after oceanic lithosphere is totally consumed, the continental portion of the same lithosphere (i.e., in the case of passive continental margins) continues to subduct to depths greater than 80 km before exhumation as a result of oceanic lithosphere broke-off at depth. The Cenozoic Himalayan and Alpine orogenies (e.g., O'Brien, 2001) and the Early Paleozoic Qilian–Qaidam orogeny (e.g. Song et al., 2006) are interpreted as examples of such processes.

Rock assemblages differ between the two end-member subduction zone scenarios. The *oceanic-type* subduction zone, such as the North Qilian suture zone, contains ophiolitic mélange (i.e., oceanic lithospheric fragments), lawsonite- or carpholite-bearing high-pressure low-temperature blueschists and eclogites (i.e., products of "cold" subduction), and an island-arc magmatic sequence (Wu et al., 1993; Song et al., 2007b; Zhang et al., 2007). The *continental-type* subduction zone, on the other hand, consists mainly of ortho- and para-gneisses, blocks of medium- to high-temperature eclogite, marble and other metasediments and garnet-bearing peridotite. The Dabie-Sulu ultrahigh-pressure metamorphic (UHPM) belt in eastern China and the North Qaidam UHPM belt of this study are type examples.

Garnet peridotite is volumetrically small yet a common component in UHPM terrenes of many *continental-type* subduction belts such as the well-studied West Gneiss Region of Norway (e.g., O'Hara and Mercy, 1963; Carswell et al., 1983; Medaris and Carswell, 1990) and the Dabie-Sulu terrane of eastern China (e.g., Yang et al., 1993; Zhang et al., 2000). This type of peridotite has received much attention for their special textures, mineral assemblages and ultradeep origin (Dobrzhinetskaya et al., 1996; van Roermund and Drury, 1998; van Roermund et al., 2001; Song et al., 2004, 2005a,b; Liu et al., 2005; Spengler et al., 2006). The observation that the orogenic garnet peridotite is exclusively associated with zones of continental collision, but is absent in zones of oceanic lithosphere subduction, has led to the suggestion of a genetic affinity of garnet peridotite with continental subduction

* Corresponding author. Address: MOE Key Laboratory of Orogenic Belts and Crustal Evolution, School of Earth and Space Sciences, Peking University, Beijing 100871, China. Tel.: +86 01 62767729; fax: +86 10 62751159.
E-mail address: sgsong@pku.edu.cn (S. Song).

1367-9120/$ - see front matter © 2008 Elsevier Ltd. All rights reserved.
doi:10.1016/j.jseaes.2008.11.009

and subsequent continental collision. In contrast, garnet-free, strongly-serpentinized peridotite is commonly believed to be restricted to *oceanic-type* subduction zones and is believed to represent the fragment of oceanic lithospheric mantle.

The North Qaidam UHPM belt is a typical *continental-type* subduction zone with characteristic rock assemblages described above (Yang et al., 2001, 2002; Song et al., 2003a,b, 2004, 2005a, 2006; Zhang et al., 2006; Mattinson et al., 2006, 2007). However, geochemical data revealed that protoliths of most of these eclogites show a broad similarity to present-day N-type and E-type MORB (Song et al., 2003b, 2006; Meng et al., 2003; Yang et al., 2006; Zhang et al., 2008). Furthermore, Song et al. (2003b) noted a strongly-serpentinized garnet-free peridotite block within bodies of eclogite with MORB-like chemistry in the North Dulan belt. Similarly, Zhang et al. (2005) reported a harzburgite block together with eclogite-facies metamorphosed ultramafic to mafic cumulate that are most consistent with being an upper mantle and lower oceanic crust ophiolitic sequence. Therefore, the presence of two types of peridotites with different tectonic histories in the North Qaidam UHPM belt warrants reconsideration of tectonic models for continental subduction, at least for the case of the North Qaidam UHPM belt.

2. Geological background

The North Qaidam UHPM belt is located between the Qilian Block in the north and Qaidam Block in the south. It trends NWW and extends from Dulan northwestward, through Xitieshan and Lüliangshan, to Yuka for about 400 km (see Fig. 1) where it is offset from the equivalent Altun UHPM belt by the Altyn Tagh Fault, a large NE-striking left-lateral strike-slip fault in western China. The Qilian Block is bound further to the north by an Early Paleozoic *oceanic-type* suture (the North Qilain suture zone) with well-exposed blueschists, eclogites and ophiolites (Wu et al., 1993; Song, 1996; Song et al., 2007a,b; Zhang et al., 2007). The North Qaidam/Altun UHPM belt mainly consists of granitic and pelitic gneisses intercalated with blocks of eclogite and varying amounts of ultramafic rocks. The rock assemblages suggest that this belt is typical of a continental-type subduction zone that differs from the "cold", *oceanic-type* subduction of the North Qilian suture zone.

Coesite and diamond inclusions have been identified in zircon grains from meta-pelite at Dulan (Yang et al., 2001, 2002; Song et al., 2003a,b) and from the garnet peridotite at Lüliangshan (Song et al., 2005a), respectively; their occurrence and *P–T* estimates of the enclosing eclogite and garnet peridotite establish the North Qaidam eclogite belt as an Early Paleozoic UHPM terrane exhumed from depths >100–200 km.

3. Occurrence and petrography

3.1. Lüliangshan garnet peridotite

The Lüliangshan garnet peridotite, first reported by Yang et al. (1994), is the only such an occurrence that has been so far recognized within the 400-km-long North Qaidam UHPM belt. It occurs as a large (~500 × 800 m in size) massif, located in Lüliangshan area, ~20 km south of the town of Da Qaidam, and is hosted within an eclogite-bearing quartzofeldspathic gneiss terrane (see Fig. 1 for its locality). This garnet peridotite massif comprises a wide range of lithologies from rocks dominated by olivine to those dominated by pyroxene. On the basis of field and petrographic observations, Song et al. (2005a, 2007a,b) grouped the rocks into four types: (1) mostly garnet lherzolite with minor amounts of (2) garnet-bearing harzburgite/dunite, (3) garnet-free dunite and (4) garnet pyroxenite dikes/dikelets (see Fig. 2 for field occurrence). Fig. 3 shows the reconstructed low-pressure (e.g., stable in the spinel peridotite field) (Niu, 1997) modes of these four rock types from their bulk-rock compositions. The garnet-free dunite plots in the harzburgite field, the garnet-bearing dunite at the boundary between harzburgite and lherzolite fields, garnet lherzolite in the fields of lherzolite and olivine websterite, and garnet pyroxenite mainly in the websterite field.

3.1.1. Garnet lherzolite

The garnet lherzolite constitutes ~70–80 vol% of the garnet peridotite massif. It is massive and coarse-grained without obvious foliations. All peridotites in the field occur as layers with varying

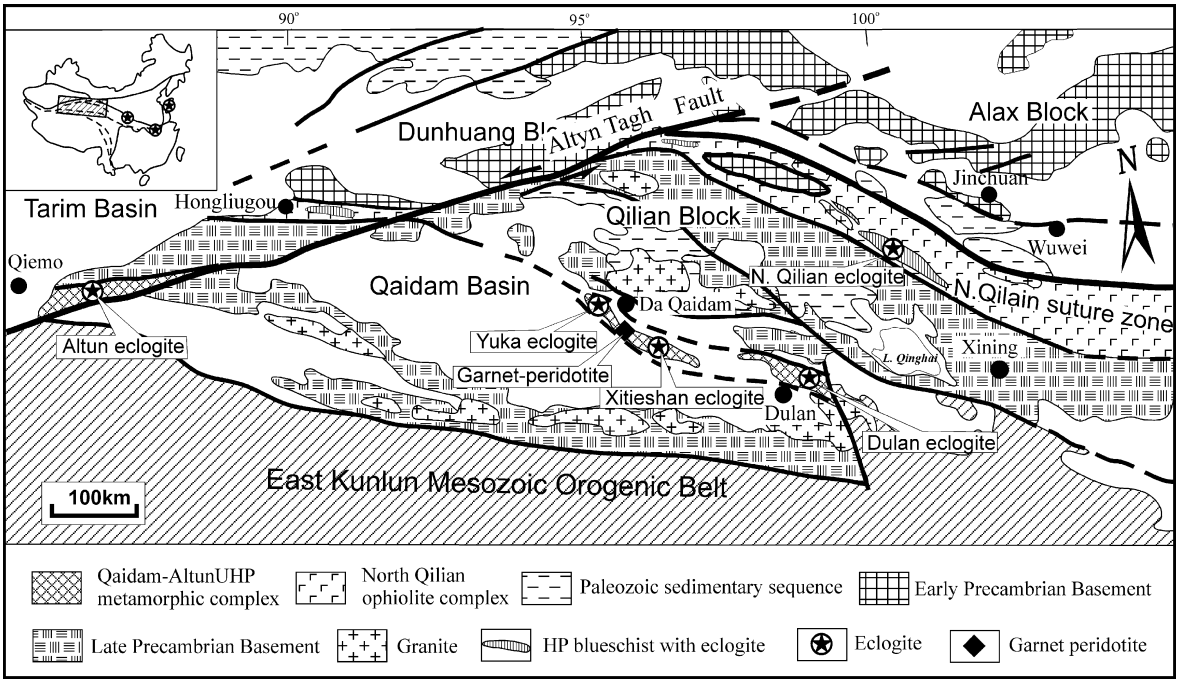

Fig. 1. Geological map of the North Tibet Plateau showing locations of eclogite and garnet peridotite of the North Qaidam UHP belt and adjacent tectonic units.

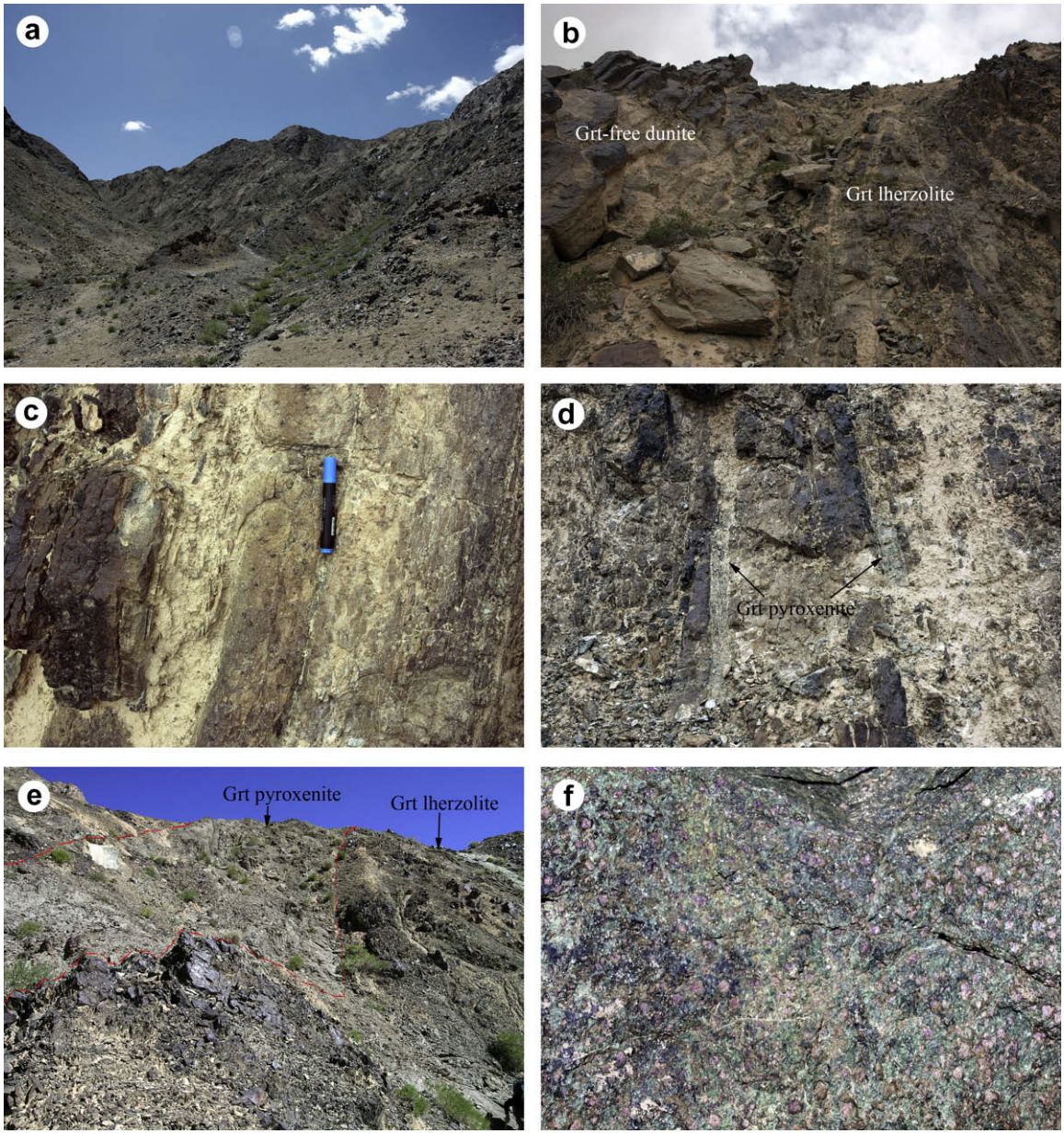

Fig. 2. Photographs showing field occurrences of various rock types of the Lüliangshan garnet peridotite. (a) Far-view of the garnet peridotite massif; (b) interbedded garnet (Grt) lherzolite and Grt-free dunite; (c) garnet lherzolite with layering structure and subsequent foliation; (d) garnet pyroxenite interbedded with garnet lherzolite; (e) garnet pyroxenite dyke cutting garnet lherzolite and (f) garnet pyroxenite with pink garnet and green clinopyroxene.

thickness (from meters to centimeters) and sharp boundaries (Fig. 2b–d). Pyroxenes vary in abundance on various scales, and thus the lithology could be termed as either garnet lherzolite or olivine websterite. The main constituent minerals are garnet, olivine, orthopyroxene (opx), clinopyroxene (cpx) and minor Cr-rich spinel (spl). Garnets are mostly porphyroblastic and vary in size (3–10 mm) and abundance (~5–15 vol%). Olivine shows a wide range of Fo values (i.e., $Mg^{\#}$, $Mg/[Mg + Fe^{2+}] = 0.84–0.91$) and constitutes 40–60 vol% of the rock. Opx and cpx take ~10–30 and 5–15 vol% of the rock, respectively. Fine-grained Cr-rich spinel ($Cr^{\#}$, $[Cr/Cr + Al] = 0.60–0.69$) is scattered fairly uniformly both in the matrix and as inclusions of major silicate minerals. Al-in-opx geobarometry (Brey and Köhler, 1990) and Grt-Ol geothermometry (O'Neill and Wood, 1979) yield $P = 5.0–6.5$ GPa and $T = 960–1040$ °C for the garnet lherzolite.

3.1.2. Garnet-bearing dunite

The garnet-bearing dunite occurs either as layers varying in thickness from 10's of cm to up to 2 m within the garnet lherzolite or as rhythmic bands that vary gradually from garnet-bearing dunite to harzburgite to garnet lherzolite. Garnet content varies widely in different layers. The rock is medium-grained and has an equigranular texture dominated by olivine ($Fo_{90.6–92.0}$) (>90 vol%), plus variable amounts of garnet, opx ($Mg^{\#} = 0.90–0.92$), and cpx ($Mg^{\#} = 0.94–0.96$). Garnets are porphyroblastic and Mg-rich (69–75 mol% pyrope, 11–18% almandine, 3–8% grossular, 0.8–2.0% spessartine and 3–6% uvarovite). Fine-grained Cr-spinel ($Cr^{\#} = 0.61–0.65$) occurs as a product of decompression-induced breakdown of previous high-Cr garnet and pyroxenes. Al-in-opx geobarometry (Brey and Köhler, 1990) and Grt-Ol geothermometry (O'Neill and Wood, 1979) yield P–T conditions of $P = 4.6–5.3$ GPa and $T = 980–1130$ °C.

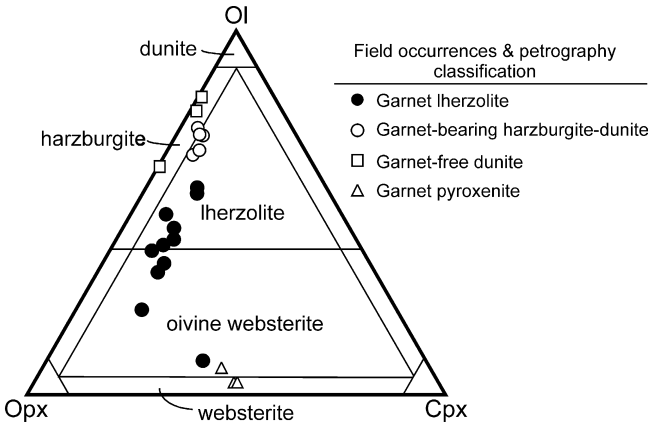

Fig. 3. IUGS rock classification (Streckeisen, 1976) of samples from the Lüliangshan metamorphic garnet peridotite using the inferred protolith mineralogy (Olivine, Opx and Cpx plus minor spinel) calculated from the bulk-rock major element compositions using the procedure developed for ultramafic rocks by Niu (1997) (after Song et al., 2007a,b).

3.1.3. Garnet-free dunite

Garnet-free dunite occurs apparently as layers and/or lenses varying in thickness of up to 10 m with brown-colored weathering surfaces distinguished from black-colored garnet lherzolite and garnet-bearing dunite (Fig. 2b). It is medium-grained, dominated by strongly-serpentinized olivine (>90 vol%) with minor opx and Cr-rich spinel. Magnetites are precipitated at the boundaries of these serpentinized olivine crystals and show a triple-junction texture. Olivine contains higher Fo contents ranging 0.924–0.937, while spinel has higher $Cr^{\#}$ (0.66–0.73) than that in garnet lherzolite.

3.1.4. Garnet pyroxenite

The garnet pyroxenite is a minor component, occurring as interlayers with the garnet peridotite (Fig. 2d), or as dikes cross-cutting the apparent layering of the massif (Fig. 2e). Most samples are fresh with pink garnet and pale-green pyroxene conspicuous in the field (Fig. 2f). The constituent phases are garnet (20–30 vol%), opx (5–10%), cpx (40–60%) and phlogopite (2–5%) with no olivine observed. It shows a fairly uniform medium-grained granular texture. The garnet is also Mg-rich (62–68 mol% pyrope, 21–24% almandine, 9.5–11% grossular, <1% spessartine, 0.8–1.5% uvarovite). It shows a fairly uniform medium-grained granular texture. Most garnets are rimmed with a kelyphitic opx + cpx + spl assemblage and some break down to granular-textured high-Al opx, cpx and Al-spl, which are characteristic decomposition features. These observations suggest that these rocks have also once equilibrated at high pressures. Their occurrences as dikelets, lack of olivine, low MgO (~18%), low $Mg^{\#}$ (~0.81), and the presence of minor phlogopite are all consistent with the garnet pyroxenite being cumulate from more evolved mantle wedge melts (Song et al., 2007a,b).

3.2. Oceanic harzburgite and cumulate in the North Qaidam UHP belt

3.2.1. Ophiolite-like sequence in Yematan section (Section A) of North Dulan belt

Garnet-free, strongly serpentinized peridotites also occur in the North Qaidam UHPM belt, as blocks of varying size. Song et al. (2003b) noted that an 80-m-thick garnet-free peridotite block occurs with garnet-bearing pyroxenite and eclogite in the Yematan cross-section (Section A in Fig. 4). The garnet pyroxenite was interpreted to be an ultramafic cumulate with high MgO (18.8 wt%), Cr (1095 ppm) and Ni (333 ppm), while eclogite blocks are geochemically similar to present-day N-type to E-type MORB. The rock assemblage most likely represents segments of an oceanic lithosphere (i.e., ophiolitic) from mantle peridotite to Mg-rich cumulate, Ca-rich gabbro, and to basaltic lavas. The garnet-free peridotite block is strongly serpentinized with no relics of primary minerals preserved.

3.2.2. Ophiolite-like sequence in Section B (Shaliuhe Section)

We have reported another large ultramafic block (~400 × 800 m in size) along the Shaliuhe cross-section (Cross-section B) in the south Dulan belt (Zhang et al., 2005, 2008). Fig. 4 shows that the northern part of Section B consists of three rock types: (1) kyanite-eclogite, (2) serpentinized harzburgite and (3) garnet-bearing pyroxenite and olivine pyroxenite. The peridotite block is dark-colored, strongly serpentinized and is apparently conformable with kyanite-eclogite and pyroxenites (Fig. 5a–c). Most samples in this peridotite block were entirely serpentinized/altered and made up of serpentine, talc, anthophyllite etc. Magnetite occurs at boundaries of olivine pseudomorphs (Fig. 5d). Relic olivine, opx/opx pseudomorphs and chromite were found in some samples (Fig. 5d–f).

The kyanite-eclogite retains a banded structure that is most probably at least partly inherited from original gabbroic cumulate bands (Fig. 6a). Geochemical analyses further reveal that this banded kyanite-eclogite has characteristics of cumulate gabbro (or more troctolitic) by high contents of Al_2O_3 (17.2–22.7 wt%), CaO (12.5–13.5 wt%), MgO (7.2–13.5 wt%), Cr (422–790 ppm), Ni, Sr, and low TiO_2 and strong positive Eu anomalies (Eu^{*} 1.51–2.08) (Zhang et al., 2008).

Olivine pyroxenite and garnet-bearing pyroxenite also show banded structure (Fig. 6b). The garnet-bearing pyroxenite has retrograded into garnet amphibolite without plagioclase. The olivine pyroxenite shows massive coarse-grained inequireanular, cumulate-like textures with olivine occurring as intercumulus between cpx grains (Fig. 6c and d). The major primary minerals are cpx, opx and olivine. The cpx is overprinted by amphibole and the opx crystals are completely replaced by amphibole and talc. These rocks are best interpreted as an Mg-rich cumulate that forms the lower part of an ophiolitic cumulate sequence.

4. Mineralogy and mineral composition of the Lüliangshan and Shaliuhe peridotites

4.1. Garnet

As already noted, the Shaliuhe Peridotite, sensu stricto, does not contain garnet. Most garnet crystals in the Lüliangshan garnet peridotite and garnet-bearing dunite are porphyroblasts with varying size (3–10 mm across). Almost all the garnet crystals exhibit kelyphitized rims of cpx, opx and spinel aggregates interpreted as resulting from decompression (Fig. 7a and b), some being completely replaced by the kelyphitic opx + cpx + spl. Pargasitic amphiboles appear at the outer circle of the kelyphite, suggesting a late retrograde metamorphic event.

High concentrations of decompression-induced exsolution products have been observed in some porphyroblastic garnet crystals including densely packed rods of rutile, cpx, opx and sodic amphibole (Fig. 7c and d). The pyroxene exsolutions suggest that their parental garnet host crystals originally possessed excess silicon, i.e., they were majoritic garnets that are only stable at depths in excess of 200 km ($P \geqslant 7$ GPa) (Song et al., 2004). The exsolution of rutile and sodic amphibole (Song et al., 2005a) further suggests that the inferred majoritic garnets also contain excess Ti, Na and hydroxyl, which are soluble in garnet only at very high pressures.

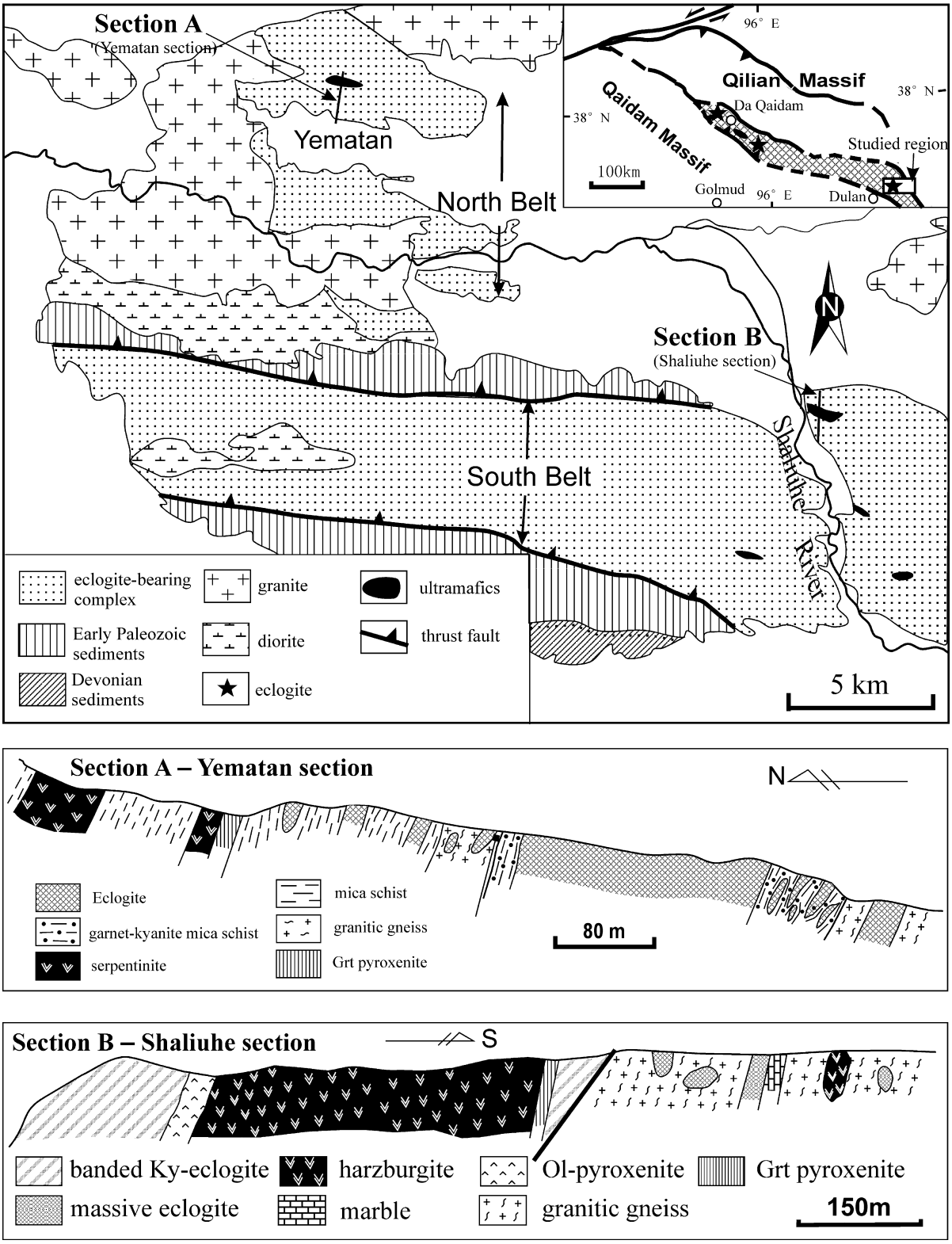

Fig. 4. Geological map of the Dulan UHP metamorphic terrane and two representative cross-sections showing fragments of eclogite-facies metamorphic ophiolite sequence.

Electron microprobe (EMP) analysis shows that garnets from garnet lherzolite and dunite are Mg-rich with a wide range of pyrope (58–74 mol%), almandine (13–25%), grossular (4–10%), spessartine (0.9–1.8%) and uvarovite (2–5%) in different samples but have a quite homogeneous composition from core to rim for a given crystal. Fig. 8 shows garnet end-member contents as a function of whole-rock $Mg^{\#}$ (i.e., $Mg/[Mg + Fe^{2+}]$). As expected, the garnet pyrope component correlates positively whereas almandine correlates negatively with the whole-rock $Mg^{\#}$, suggests that garnet is in equilibrium with coexisting minerals in the rock (Fig. 8).

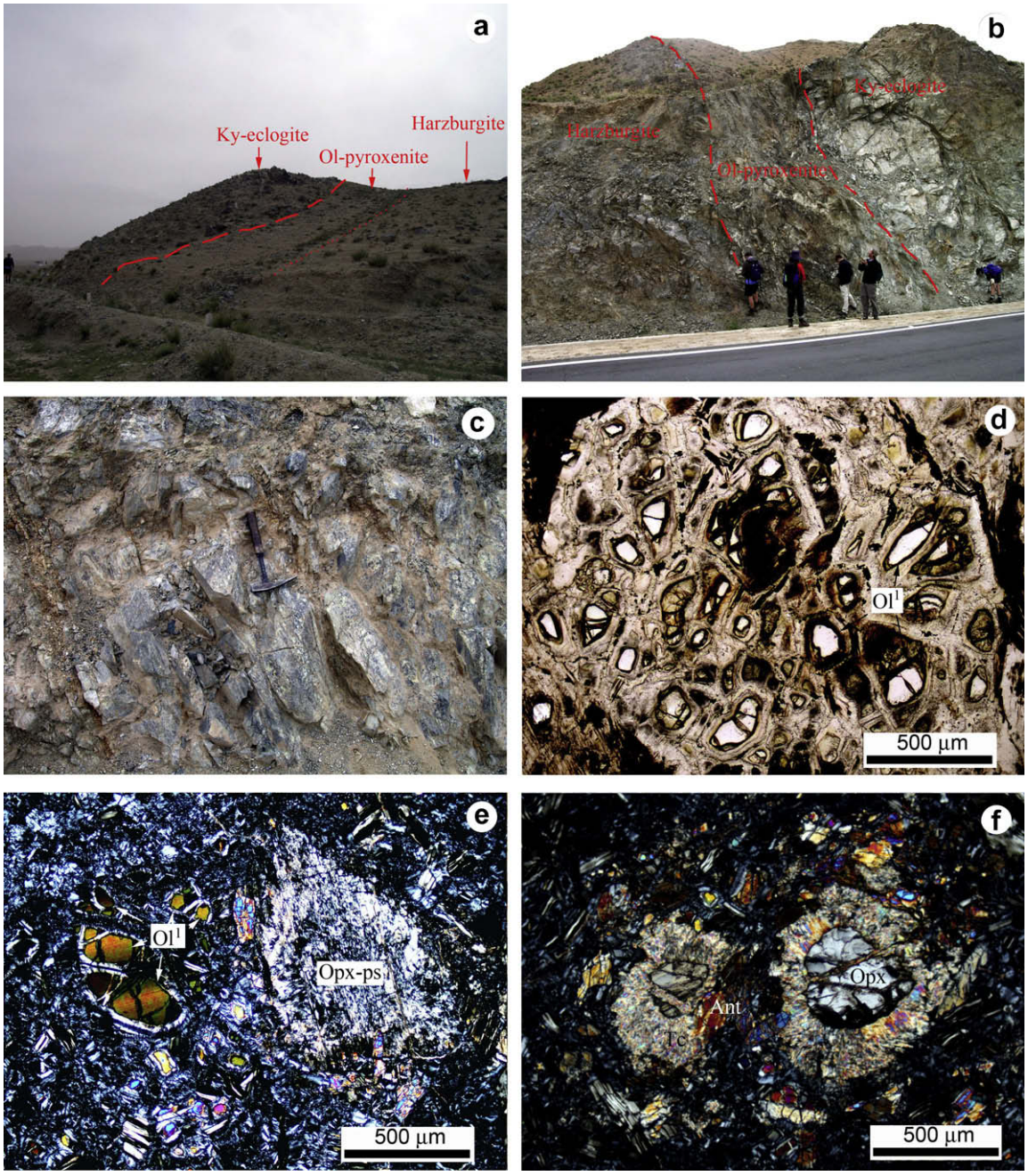

Fig. 5. Photographs showing ophiolitic harzburgite and cumulate in the Shaliuhe cross-section. (a) Field occurrence of serpentinized harzburgite, banded kyanite (Ky)-eclogite and olivine pyroxenite in the north end of the Shaliuhe section. (b) Field occurrence of serpentinized harzburgite, banded kyanite (Ky)-eclogite and garnet pyroxenite in the middle part of the Shaliuhe section. (c) Serpentinized harzburgite. (d–f) Photomicrographs showing relic olivine (Ol^1) and orthopyroxene (Opx) and its pseudomorphs (Opx-ps).

4.2. Olivine

4.2.1. Olivine from the Lüliangshan garnet peridotite

Olivine from the Lüliangshan garnet peridotite shows a large compositional variation in terms of Fo content (i.e., $Mg^{\#}$ of olivine), which correlates positively with modal percentage of olivine. Olivine in garnet-free dunite has the highest Fo content of 0.927–0.937, which is slightly higher than that of garnet-bearing dunite (0.906–0.926). Fo content of olivine in garnet lherzolite, on the other hand, varies from 0.830 to 0.906. NiO concentrations vary from 0.34 to 0.55 wt%.

Ilmenite and Al-chromite rod- and needle-shaped exsolutions have been observed in some large olivine crystals (Fig. 7e and f), and are interpreted as resulting from decompression of the same phases previously dissolved in olivine structures stable at great depths of 200 km (Song et al., 2004).

4.2.2. Olivine from the Shaliuhe harzburgite and olivine pyroxenite

Two generations of olivine have been recognized in the Shaliuhe peridotite (Zhang et al., 2005): relic olivine (Ol^1) and metamorphic olivine (Ol^2). The first generation of olivine (Ol^1) occurs as small relic crystals among serpentines, and some crystals retain clear kink-bands (Fig. 5e). EMP analysis shows that the relic olivine has a narrow range of Fo content from 0.883 to 0.915 and relatively high NiO content from 0.28 to 0.46, which is consistent with the olivine compositions from the present-day abyssal peridotite (Fig. 9a). The

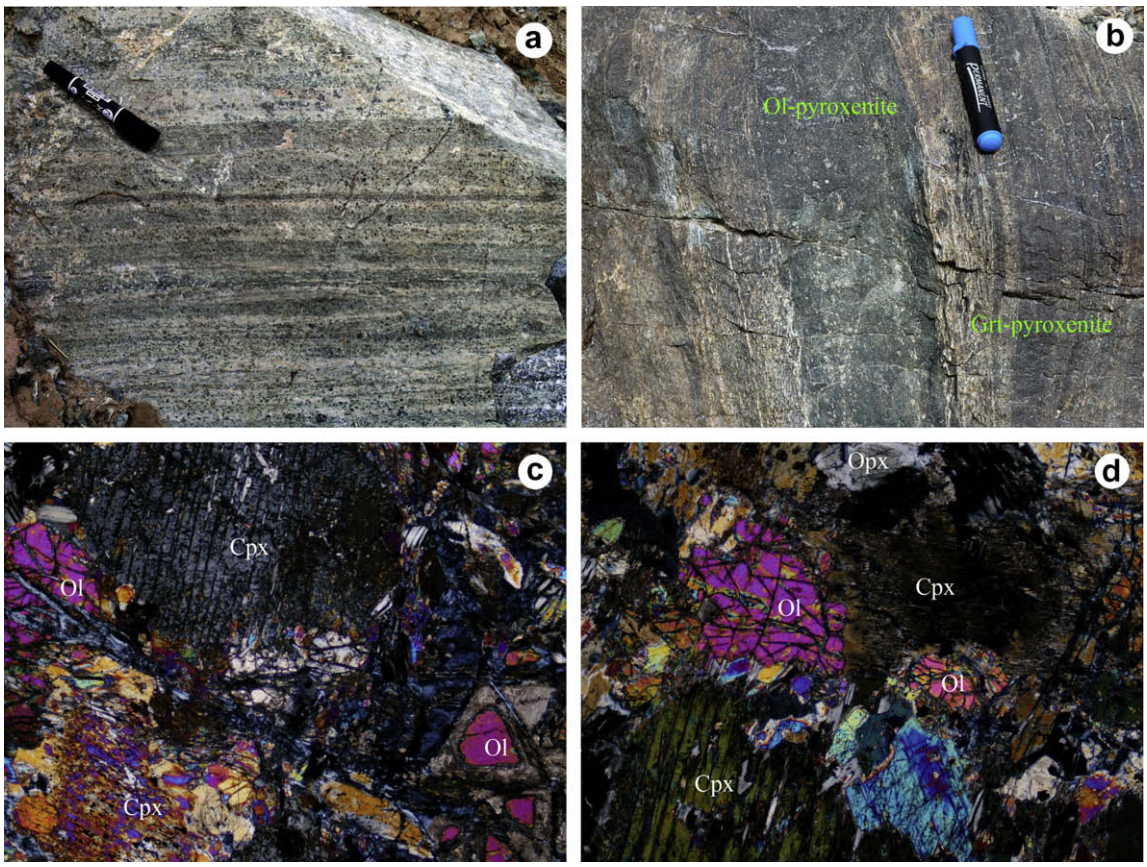

Fig. 6. Photographs of cumulate units of the Shaliuhe ophiolite sequence. (a) Banded structure of kyanite-eclogite. (b) Banded structure of garnet-bearing and olivine pyroxenites. (c and d) Micro-texture of olivine pyroxenite showing relation between olivine (Ol) and pyroxenes.

second generation (Ol^2) occurs as large and dirty crystals with a dense cluster of tiny fluid inclusions. EMP analysis shows these olivines have extremely high Fo content of 0.943–0.966 but low NiO content (0.21–0.35 wt%) (Fig. 9a), which is consistent with an origin through recrystallization of serpentines during subsequent metamorphism (i.e., eclogite-facies?; Zhang et al., 2008). Olivine in the cumulate olivine pyroxenite has a narrow Fo range (0.88–0.90) and low NiO content (0.25–0.39 wt%).

4.3. Orthopyroxene

Opx in the Lüliangshan garnet peridotite also shows a large compositional variation in terms of $Mg^{\#}$ (Fig. 9b). Opx from garnet-bearing dunite has high $Mg^{\#}$ (0.94–0.96) whereas opx from garnet lherzolite has significantly lower $Mg^{\#}$ (0.87–0.93). Opx $Mg^{\#}$ values are positively correlated with Fo values of coexisting olivine. All opx crystals in the Lüliangshan garnet peridotite (including garnet lherzolite and garnet-bearing dunite) are extremely depleted in Al_2O_3. Al_2O_3 in opx from lherzolite is low (0.38–0.66 wt%), and is slightly higher in dunite (0.55–0.73 wt%). Opx crystals from garnet pyroxenite have lower $Mg^{\#}$ (0.86–0.90) and higher Al_2O_3 (0.88–1.17 wt%) than those from garnet peridotite.

High concentrations of decompression-induced exsolution needles were observed in some porphyroblastic opx (Fig. 10a). Energy-dispersive X-ray spectrometer (EDS) scanning reveals that those needles are Cr-rich spinel, suggesting that the original host opx was rich in Cr content.

Opx in the Shaliuhe harzburgite, on the other hand, occurs as relic crystals surrounded by talc (Tc) + anthophyllite (Ant) corona (Fig. 5f) and some occur as opx pseudomorphs completely replaced by talc and serpentine (Fig. 5e). High concentrations of cpx lamellae occur in the relic opx crystals, suggesting high CaO-content in the original host opx (Fig. 10b and c) that should be stable at magmatic conditions (>1100 °C, Lindsley, 1983; Niu, 1999). EMP analysis shows that opx from the Shaliuhe harzburgite has high Al_2O_3 (2.69–4.63 wt%) and high and constant $Mg^{\#}$ (0.908–0.917), which is within the compositional range of opx from present-day abyssal peridotites, but differs from opx in the Lüliangshan garnet peridotite (Fig. 9b).

4.4. Clinopyroxene

Cpx crystals in the Lüliangshan garnet peridotite are rich in Cr_2O_3 (0.6–1.6 wt%). High concentration of quartz, amphibole and Cr-rich spinel exsolution rods/lamellae in some cpx crystals (Fig. 10d) are interpreted as resulting from decompression (Song et al., 2004), which points to originally high-Si and Cr cpx at peak metamorphic conditions. Cpx $Mg^{\#}$ varies from 0.91 to 0.96 and is positively correlated with $Mg^{\#}$ of olivine and opx. Al_2O_3 varies from 1.13 to 3.19 wt%, and Na_2O from 0.43 to 1.32 wt%.

Cpx in the Shaliuhe harzburgite occurs only as exsolution lamellae in opx crystals described above. No cpx relic crystals or pseudomorphs are observed in the Shaliuhe harzburgite. Cpx crystals do occur in the Shaliuhe cumulates (garnet-bearing pyroxenite and olivine pyroxenite) and have very high CaO (24.8–25.1 wt%).

4.5. Spinel

Spinel crystals in the Lüliangshan garnet peridotite are secondary and occur as fine-grained (5–100 μm) euhedral crystals scattered fairly uniformly both between, and as inclusions of, major

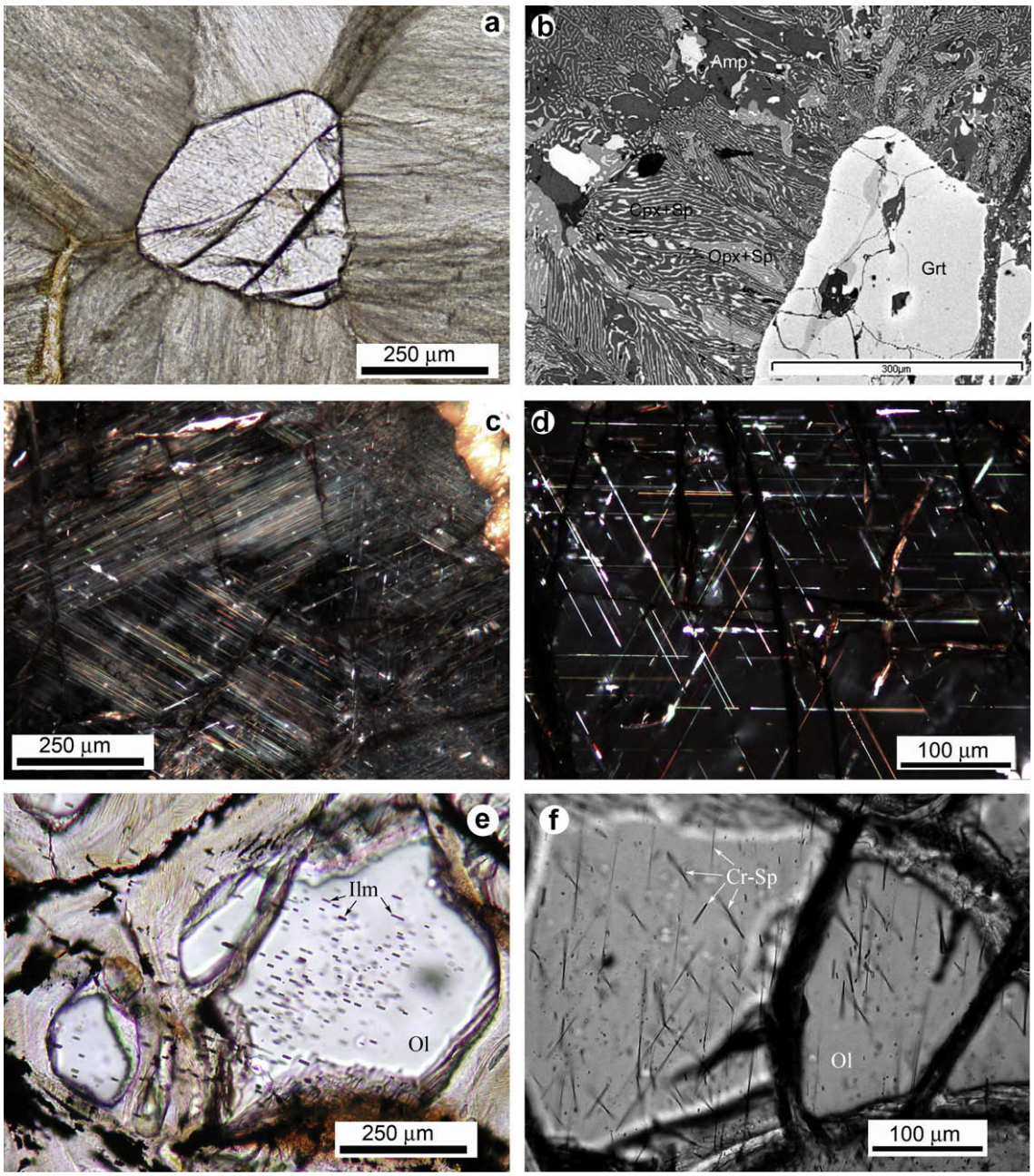

Fig. 7. Photomicrographs of garnet and olivine from the Lüliangshan garnet peridotite. (a) Kelyphite texture around garnet crystal. (b) Back-scattered electron image for kelyphite texture around garnet. (c and d) Rutile + sodic amphibole exsolution lamellae in garnet crystals. (e) Ilmenite exsolution rods in olivine from the Lüliangshan garnet peridotite. (f) Cr-spinel exsolution needles that show four directions in olivine from the Lüliangshan garnet peridotite.

silicate minerals in garnet lherzolite and garnet-bearing dunite, or occur as exsolved lamellae in porphyroblastic olivine and cpx (Song et al., 2004, 2007a,b). $Cr^{\#}$ (Cr/[Cr + Al]) of the spinel varies from 0.54 to 0.73 and correlates positively with whole-rock $Mg^{\#}$ (Song et al., 2007a,b).

No Al-rich spinel but some chromite crystals are found in the Shaliuhe harzburgite.

5. Discussion

The petrogenesis of peridotite blocks in *continental-type* UHPM belts has long been discussed (Carswell et al., 1983; Medaris and Carswell, 1990; Zhang et al., 1994, 2000; Brueckner, 1998; Liou and Carswell, 2000; Medaris, 1999; Brueckner and Medaris, 2000). Much of the discussion, however, has focused on deep origins of garnet-bearing peridotites, whereas garnet-free, intensively serpentinized peridotite blocks are usually neglected. Protoliths of eclogites and ultramafic rocks in most UHPM terranes, such as the Dabie-Sulu of eastern China (Jahn, 1999) and Western Gneiss Region of Norway (Carswell et al., 2003), are believed to be the original mafic/ultramafic complexes hosted in the gneisses of the continental crust or fragments of the mantle wedge before and during continental subduction.

5.1. Petrogenesis of the Lüliangshan garnet peridotite

By interpreting hydrous minerals in olivine, cpx, and garnet as "inclusions", Yang and Powell (2008) suggested that the Luliang-

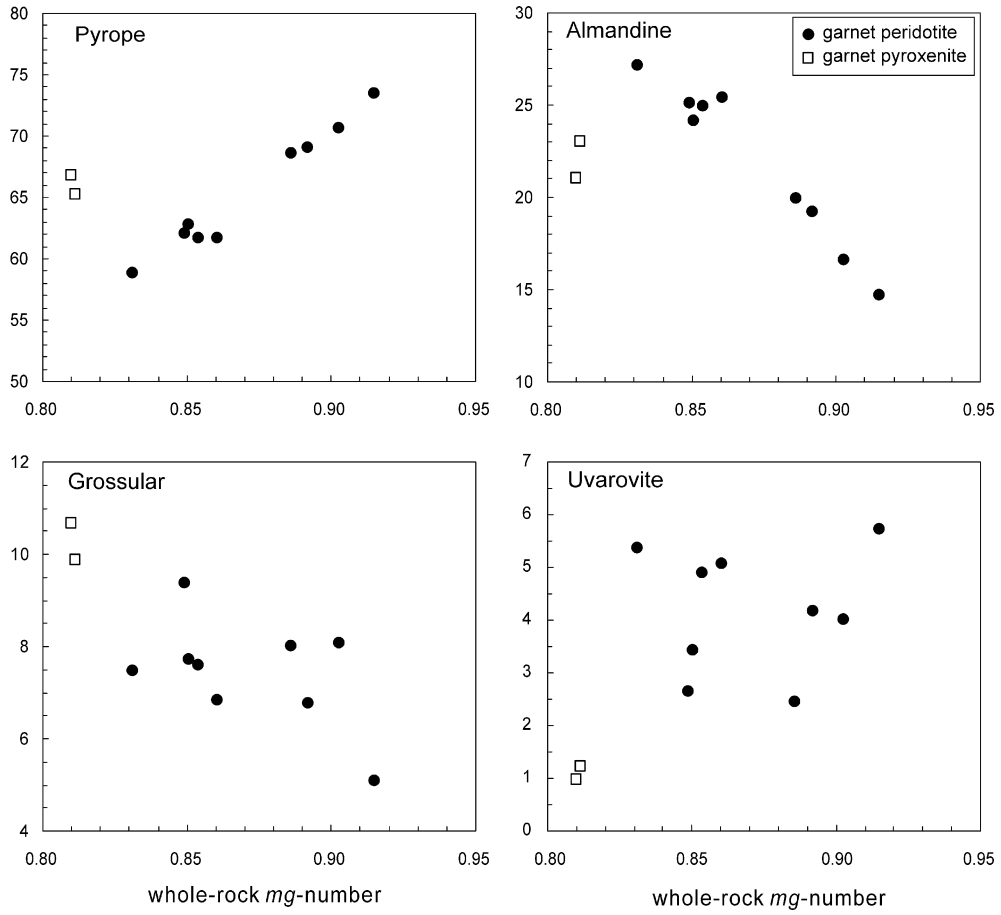

Fig. 8. Diagrams showing end-member contents of garnets from various rocks in correlation with Mg-number of whole-rock composition.

shan garnet peridotite was formerly mantle peridotite emplaced into the oceanic crust followed by serpentinization near the sea floor. They interpreted that these serpentinites were later transformed into garnet lherzolite and dunite during subduction to conditions of 3.0–3.5 GPa and 700 °C. The speculation by Yang and Powell (2008) differs from our previous studies (Song et al., 2004, 2005b, 2007a,b). The key difference lies in the interpretation of whether the hydrous minerals present in the aforementioned minerals are true "inclusions" or decompression products and their altercations.

This phenomenon described above is ubiquitous in the strongly-serpentinized Luliangshan peridotite. The stronger retrograde/serpentinization the sample has experienced, the more these hydrous phases are present in garnet, olivine and pyroxenes. As shown in Figs. 3 and 4 of Yang and Powell (2008), samples are strongly serpentinized and all "inclusions" are surrounded by cracks. Therefore, petrographic observation suggests that their so-called "inclusions" in garnet and olivine are actually not inclusions, but subsequent retrograde decompression/alteration products. Furthermore, both structure and mineral assemblage their "inclusions" in garnet are actually the same as the outer-rim symplectite, which suggests a rather late-stage decompression of garnet. Also, lizardite and antigorite are polymorphs of serpentines with the same composition but different structure. Their occurrence is closely associated with degrees of serpentinization, that is, lizardite usually occurs in the first stage of serpentinization, and antigorite appears as the degree of serpentinization increases (Deer et al., 1992). This should explain why the lizardite occurs as "inclusions" in olivine or cpx and antigorite in the matrix. Importantly, serpentinization always releases iron to form magnetite/chromite, but the iron is difficult to re-enter the olivine's structure during metamorphism. Therefore, the metamorphic olivine from former serpentine should have very high Fo contents (for example, metamorphic olivine with Fo 94–97 in the Shaliuhe oceanic harzburgite, see above). If the Qaidam garnet peridotite was metamorphosed from a former serpentinized body, all olivines in the matric (but not the relic inclusion) should have very high Fo values (>95 mol%), but this is not the case. In fact all the olivines have a wide Fo range from 83 to 93. It is also noteworthy that major mineral and whole-rock compositions in different rock types reveal that the Qaidam garnet peridotite is not an abyssal peridotite but an ultramafic cumulate (see below).

Whole-rock and mineral compositions show that the garnet peridotite massif from the North Qaidam UHPM belt resembles "Mg–Cr type" of Carswell et al. (1983). Field occurrences of these various rock types show obvious layering largely defined by modal variations of major constituent minerals (Grt, olivine, opx and cpx). Rhythmic crystallization bands of the protoliths can be inferred with confidence in the field. The interlaying relationship between garnet-bearing dunite and garnet lherzolite is also clear on the outcrop. Both field observations and the estimated low-pressure (spinel peridotite stability depths or shallower) modal mineralogy (Fig. 3) suggest that protoliths of the garnet-free dunite and garnet-bearing harzburgite may indeed have been harzburgite, probably representing the sub-arc lithospheric mantle (see below).

However, the protoliths of garnet lherzolite and garnet pyroxenite were likely magmatic cumulates, consistent with trace element systematics (Song et al., 2007a). They encompass a wide range of rock compositions equivalent to low-pressure magmatic cumulate assemblages of websterite, olivine websterite and lherz-

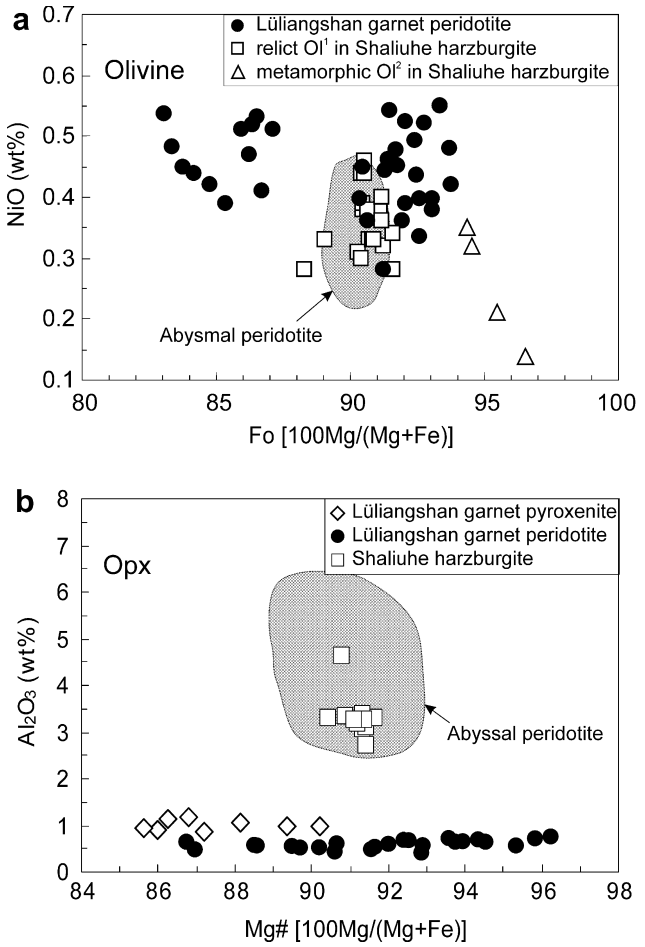

Fig. 9. Compositional variations of olivines (a) and orthopyroxenes (b) from the two types of peridotite in the North Qaidam UHP belt, in comparison with olivines from present-day abyssal peridotite (shadowed field) (Dick, 1989). Fo content of olivines from the Luliangshan garnet peridotite massif varies in a wide range from 83.0 to 93.7 mol%, whereas relic olivines (Ol^1) from the Shaliuhe harzburgite in a narrow range from 88.3 to 91.5 mol%, in consistent with abyssal peridotite and olivines (Ol^2) metamorphosed from the former serpentine have high Fo content from 94.3 to 96.6.

olite. Such a large whole-rock compositional variation could be due to sample size variation, large grain size and modal heterogeneity, but the overall increase in bulk-rock $Mg^{\#}$ with increasing modal olivine is consistent with their protoliths being of cumulate origin. This is a strong argument.

Given the fact that the garnet porphyroblasts are clearly of post-magmatic metamorphic origin and that olivine has variable Fo ($Mg^{\#}$ = 0.830–0.937), we can infer that protoliths of the lherzolite were ultramafic cumulates from a cooling melt of basaltic composition ($Mg^{\#}$ = 0.558–0.748) (Niu et al., 2002). The major and trace element characteristics of these rocks (Song et al., 2007a,b) indicate that the mantle melts were probably subduction-zone associated mantle wedge melts. The emplacement depth of the cumulate is hard to evaluate, but probably occurred in the sub-arc lithosphere where the mantle wedge-derived melts experienced cooling and crystallization. The harzburgite, inferred to be protoliths of the garnet-free dunite and garnet-bearing harzburgite, may in fact have been *in situ* lithospheric mantle that hosted the melts.

The circumstantial lines of evidence in support our inference include: (1) all rocks show relative depletion of HFSEs (Nb, Ta, Zr, Hf and Ti) and enrichment of LILEs with spikes of fluid-mobile elements (e.g., Cs, U, Pb and Sr), which are typical geochemical signatures of subduction magmatism (e.g., Elliott et al., 1997; Ewart et al., 1998); (2) high-MgO parental melts, estimated from the $Mg^{\#}$ of garnet-bearing dunite, suggest that they may have been sourced from more depleted mantle, probably the depleted sub-arc asthenosphere; (3) cores of magmatic zircons in the garnet lherzolite samples yield an age of 457 ± 22 Ma (Song et al., 2005b), which represents the time of subduction-zone associated mantle wedge magma genesis, and is consistent with the metamorphic ages of the ~458 Ma (zircon SHRIMP and Sm/Nd bulk-rock mineral isochron ages) eclogites of MORB/OIB protoliths from the same UHPM belt (Song et al., 2003a,b, 2006) and (4) all the three major rock types (except for garnet-free dunite) show weak to none negative Eu^{*}-anomaly (Song et al., 2007a,b), suggesting that plagioclase was originally absent during crystallization of their protoliths. Assuming that the peridotite massif, i.e., protoliths of the garnet lherzolite and garnet pyroxenite, were indeed of cumulate origin from a cooling melt, the estimated liquidus temperature would have been 1170–1250 °C with a mean of ~214 ± 32 °C (Niu et al., 2002). Such relatively low liquidus temperatures (low $Mg^{\#}$ of the minerals and the bulk-rock compositions) argue for basaltic (vs. ultramafic) parental melts. Given that the liquidus phases are dominated by olivine and cpx (perhaps also opx) without plagioclase (too low Al_2O_3 and CaO in the bulk-rock compositions), we can infer that the melts were rich in water that suppressed plagioclase but enhanced cpx on the liquidus (Gaetani et al., 1993; Niu, 2005). Such conditions are less likely beneath normal ocean ridges, but readily satisfied in a mantle wedge overlaying a subduction zone.

5.2. Petrogenesis of the oceanic-type harzburgite

As discussed above, the oceanic-type harzburgites in the North Qaidam UHP belt are closely associated with eclogite-facies metamorphosed ultramafic to gabbroic cumulates, which allows us to infer that these rock types constitute the lower most sections of an oceanic lithospheric sequence. Fo in the relic olivine and Al_2O_3 in the relict opx are significantly different from those in the Lüliangshan garnet peridotite, but are very similar to present-day abyssal harzburgites, suggesting that the oceanic-type harzburgite represents mantle peridotite of the subducted oceanic lithosphere.

The presence of the second generation of high-Fo (Fo = 94–97 mol%) olivines (Ol^2) suggests that the serpentinized harzburgite experienced a metamorphic event in which the serpentines were re-metamorphosed into olivine. This metamorphic event was most probably associated with medium to high-temperature metamorphism during continental subduction, because during cold oceanic subduction serpentine would be a stable phase and would not be re-crystallized to olivine. The absence of garnet in the re-metamorphosed harzburgite is most probably caused by the low-Al_2O_3 bulk composition despite the ultrahigh-pressure condition.

5.3. Ages of the Lüliangshan garnet peridotite

Three major age groups have been determined by zircon U–Pb SHRIMP geochronological studies from the Lüliangshan garnet lherzolite, garnet-bearing dunite and garnet pyroxenite (Song et al., 2005a). (1) Cores of most crystals, whose oscillatory zoning morphology and rare earth element (REE) systematics (i.e., very high $[Lu/Sm]_{CN}$ = 88–230) suggest a magmatic origin, yielded ages of 484–444 Ma (weighted mean age, 457 ± 22 Ma), consistent with the magmatic cumulate origin of their protoliths. (2) The mantle portions of zircon crystals that contains inclusions of garnet, pyroxene, olivine and diamond gave ages of 435–414 Ma with a mean of 423 ± 5 Ma, and are therefore interpreted to record the time of ultrahigh-pressure metamorphism (UHPM) at depths greater than 200 km in a *continental-type* subduction zone. (3)

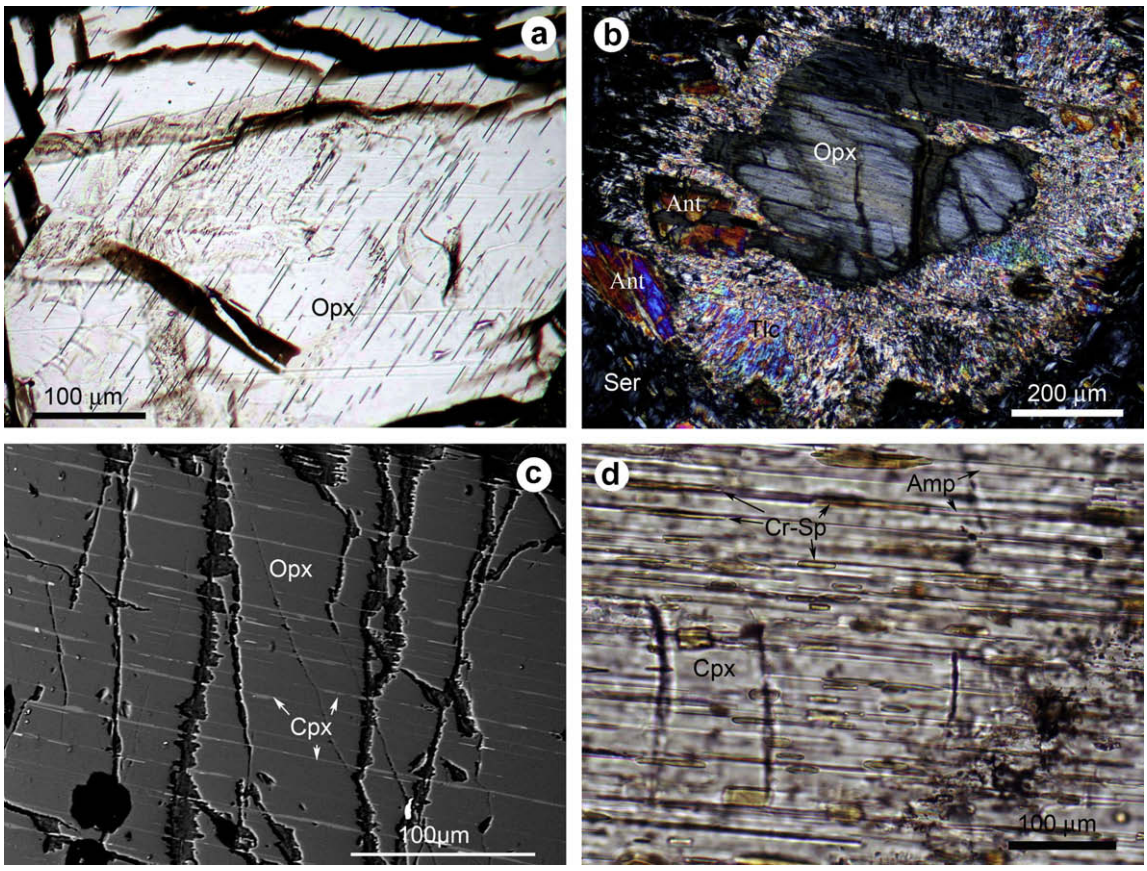

Fig. 10. Photomicrographs of pyroxenes from two types of peridotite in the North Qaidam UHP belt. (a) Ilmenite needles exsolved from orthopyroxene (Opx) from the Lüliangshan garnet peridotite; (b) relic Opx surrounded by talc (Tc) + anthophyllite (Ant) corona from the Shaliuhe harzburgite; (c) BSE image showing Cpx lamellae exsolved from relic Opx from the Shaliuhe harzburgite and (d) Cr-spinel + amphibole (Amp) exsolution rods in Cpx from the Lüliangshan garnet peridotite.

The near-rim portions of zircon crystals yielded ages of 402–384 Ma (mean age 397 ± 6 Ma), which are thought to represent the retrograde event during exhumation.

5.4. Ages of the Shaliuhe ophiolite suit

The oceanic harzburgites, on the other hand, have no zircons because of their highly depleted compositions. Therefore, it is difficult to determine both magmatic and metamorphic ages of the harzburgite itself. Field relationship between the harzburgite and the associated UHP ultramafic to mafic cumulates (including Ky-eclogite in the Shaliuhe cross-section) and the OIB- and MORB-affinity of the eclogite suggests they belonged to an ophiolitic succession (Song et al., 2003a,b; Zhang et al., 2005, 2008). Eclogites in the north Dulan sub-belt give SHRIMP zircon U–Pb age of 457 ± 7 Ma (Song et al., 2006) and garnet-omphacite-whole-rock Sm–Nd ages of 458 ± 10 Ma and 459 ± 3 Ma (Song et al., 2003a,b), suggesting that eclogite-facies metamorphism occurred at ~460 Ma, which was overprinted to various extents by late-stage (UHP?) metamorphism (Song et al., 2003a,b; Mattinson et al., 2006).

SHRIMP U–Pb dating, in combination with cathodoluminescent (CL) imaging analysis, reveals that zircon separates from a banded kyanite-eclogite sample in the Shaliuhe section have three groups of ages (Zhang et al., 2008). The relic cores from nine zircon grains yield ages of 500–549 Ma, which, marked with magmatic oscillatory zoning and high Th/U ratios (0.98–1.38), should represent the time of cumulate crystallization beneath the inferred ocean ridge and therefore date the formation age of the ophiolite suite. Fourteen analyses of the metamorphic mantle portions of the zircon grains give ages ranging from 484 Ma to 436 Ma with a mean at 450 ± 7 Ma and five bright luminescent rims yield ages of 424–430 Ma with a mean at 426 Ma.

The UHP metamorphic ages of the North Qaidam UHPM belt were further corroborated by SHRIMP ages of coesite-bearing zircon grains from the pelitic gneisses (423 ± 6 Ma, Song et al., 2006) and diamond-bearing metamorphic zircon grains from the Lüliangshan garnet lherzolite and garnet-bearing dunite (423 ± 5 Ma, Song et al., 2005b). These ages are consistent with the metamorphic ages of eclogite samples (422–432 Ma, Mattinson et al., 2006). The exhumed garnet peridotites clearly experienced mantle depths in excess of 200 km, whereas the exhumed granitic/pelitic gneisses (supra-crustal rocks) and eclogites would seem to have reached mantle depths no less than ~100 km. The differences in both metamorphic ages and pressure conditions may provide clues concerning the history of oceanic lithosphere subduction, continental subduction/collision, and ultimate exhumation in the northern margin of the Tibetan Plateau in the Paleozoic.

5.5. Tectonic evolution of the two types of peridotites

Petrological and geochemical data, together with age data, reveal that some of the protoliths of the bulk Lüliangshan garnet peridotite within the North Qaidam UHP belt are of cumulate origin from a high-Mg magma in an arc environment. Ultrahigh-pressure metamorphism of the garnet peridotite to depths greater than 200 km was closely associated with the subduction of the enclosing continental crust. On the other hand, the presence of Early

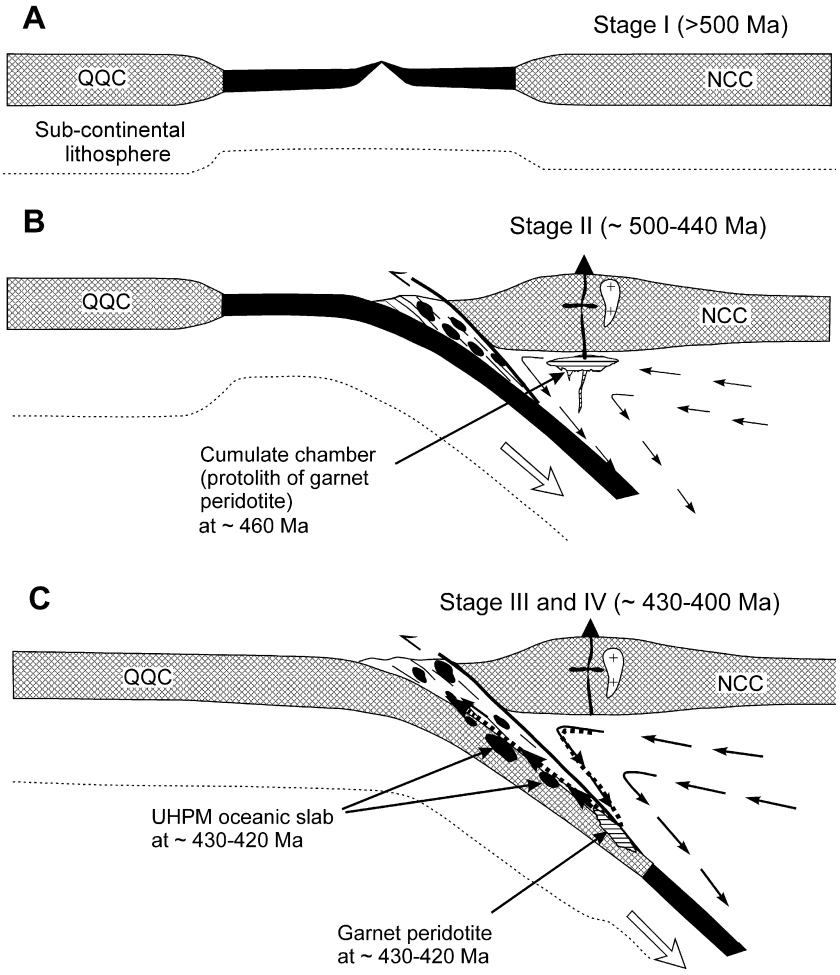

Fig. 11. A tectonic modal that illustrates the forming process and environment for the two types of peridotite in the North Qaidam UHP belt (modified after Song et al., 2007a,b). (A) Generation of the Qilian oceanic lithosphere between the Qaidam–Qilian block and the North China Craton at ages >500 Ma. (B) Subduction of North Qilian Ocean that formed the eclogitilated ophiolite slab in subduction zone and sub-arc cumulate chamber in the volcanic arc environment at about 460 Ma. (C) Corner flow of the mantle wedge during continental subduction has dragged both the ophiolite slab and the cumulate down to depths about 100–200 km at about 430–420 Ma and exhumed during subsequent continental collision (~400 Ma).

Paleozoic oceanic harzburgite and ophiolite suits within the North Qaidam rocks demonstrates the likelihood of oceanic subduction prior to the continental subduction and collision. If these bodies are indeed derived from oceanic lithosphere (both crustal and mantle sections), it would suggest that at least some eclogite and peridotite blocks within gneisses may not be "*in situ*". Therefore, we propose a four-stage tectonic evolution model for the two types of peridotite blocks in the North Qaidam UHPM belt. Stage I (~549−500 Ma): The oceanic lithosphere of the "Qilian Ocean" were spreading and started to subduct between the Qaidam–Qilian block, a fragment of the Rodinia super-continent, and the North China Craton (Fig. 11a). Stage II (~460 Ma): Eclogite-facies metamorphism and dehydration of subducted oceanic lithosphere (eclogite-facies metamorphic stage, Song et al., 2006; Mattinson et al., 2006) caused mantle wedge partial melting and high-Mg melt generation in a sub-arc environment; cooling-induced crystallization of these melts led to the formation of the cumulate assemblage in the sub-arc lithospheric mantle in the spinel peridotite stability field at about 460 Ma (Fig. 11b). Stage III: The subducting oceanic lithosphere slab induced mantle wedge corner flow that transported the cumulate peridotite body deep into the mantle in the subduction zone. Stage IV: The subsequent subduction of continental crust captured the peridotite body and carried it to depths in excess of 200 km where it underwent UHP metamorphism at about 420–430 Ma before being exhumed with the supracrustal felsic gneisses to the middle-crust level at about 400 Ma (Fig. 11c).

Acknowledgements

We thank Hannes Brueckner and Ruth Y. Zhang for their constructive review comments, which led to a better presentation of the final product. This study was supported by National Natural Science Foundation of China (Grant Nos. 40773012, 40825007, 40572045), the Foundation for the Author of National Excellent Doctoral Dissertation of China (200531), the Major State Basic Research Development Projects (2009CB825007) and by the science foundation of State Key Laboratory of Geological Processes and Mineral Resources, China University of Geosciences (GPMR200632).

References

Brey, G.P., Köhler, T., 1990. Geothermobarometry in four-phase lherzolites II. New thermobarometers, and practical assessment of existing thermobarometers. Journal of Petrology 31, 1353–1378.

Brueckner, H.K., 1998. Sinking intrusion model fro the emplacement of garnet-bearing peridotites into continent collision orogens. Geology 26, 631–634.

Brueckner, H.K., Medaris, L.G., 2000. A general model for the intrusion and evolution of 'mantle' garnet peridotites in high-pressure and ultra-high-pressure metamorphic terranes. Journal of Metamorphic Geololy 18, 123–133.

Carswell, D.A., Harvey, M.A., Al-Samman, A., 1983. The pretogenesis of contrasting Fe–Ti and Mg–Cr garnet peridotite types in the high grade gneiss complex of western Norway. Bulletin of Mineralogy 106, 727–750.

Carswell, D.A., Brueckner, H.K., Cuthbert, S.J., Mehta, K., O'Brien, P.J., 2003. The timing of stabilisation and the exhumation rate for ultra-high pressure rocks in the Western Gneiss Region of Norway. Journal of Metamorphic Geology 21, 601–612.

Deer, W.A., Howie, R.A., Zussman, J., 1992. The Rock Forming Minerals, second edition. John Wiley & Sons Inc., New York, 696pp.

Dick, H.J.B., 1989. Abyssal periodotites, very slow spreading ridges and ocean ridge magmatism. In: Saunders, A.D., Norry, M.J. (Eds.), Magmatism in the Ocean Basins. Geological Society, London, Special Publications, 42, 71–105.

Dobrzhinetskaya, L., Green, H.W., Wang, S., 1996. Alpe Arami: a peridotite massif from depths of more than 300 kilometers. Science 271, 1841–1845.

Elliott, T., Plank, T., Zindler, A., White, W., Bourdon, B., 1997. Element transport from slab to volcanic front at the Mariana Arc. Journal of Geophysics Research 102, 14991–15019.

Ernst, W.G., 2001. Subduction, ultrahigh-pressure metamorphism, and regurgitation of buoyant crustal slices – implications for arcs and continental growth. Physics of the Earth and Planetary Interiors 127, 253–275.

Ewart, A., Collerson, K.D., Regelous, M., Wendt, J.I., Niu, Y., 1998. Geochemical evolution within the Tonga-Kermadec-Lau Arc-Backarc system: the role of varying mantle wedge composition in space and time. Journal of Petrology 39, 331–368.

Gaetani, G.A., Grove, T.L., Bryan, W.B., 1993. The influence of water on the petrogenesis of subduction-related igneous rocks. Nature 365, 332–334.

Jahn, B.-M., 1999. Sm–Nd isotope tracer of UHP metamorphic rocks: implications for continental subduction and collisional tectonics. International Geology Review 41, 859–885.

Lindsley, D.H., 1983. Pyroxene thermometry. American Mineralogist 68, 477–493.

Liou, J.G., Carswell, D.A., 2000. Preface: garnet peridotites and ultrahigh-pressure minerals. Journal of Metamorphic Geology 18, 121.

Liu, L., Chen, D.L., Zhang, A.D., Sun, Y., Wang, Y., Yang, J.X., Luo, J.H., 2005. Ultrahigh pressure (>7 GPa) gneissic K-feldspar (-bearing) garnet clinopyroxenite in the Altyn Tagh, NW China: evidence from clinopyroxene exsolution in garnet. Science in China Series D – Earth Sciences 48 (7), 1000–1010.

Maruyama, S., Liou, J.G., Terabayashi, M., 1996. Blueschists and eclogites of the world and their exhumation. International Geology Review 38, 485–594.

Mattinson, C.G., Wooden, J.L., Liou, J.G., Bird, D.K., Wu, C.L., 2006. Age and duration of eclogite-facies metamorphism, North Qaidam HP/UHP terrane, western China. American Journal of Science 306, 683–711.

Mattinson, C.G., Menold, C.A., Zhang, J.X., Bird, D.K., 2007. High- and ultrahigh-pressure metamorphism in the North Qaidam and South Altyn Terranes, western China. International Geology Review 49, 969–995.

Medaris, L.G., 1999. Garnet peridotites in Eurasian high-pressure and ultrahigh-pressure terranes: a diversity of origins and thermal histories. International Geology Review 41, 799–815.

Medaris, L.M., Carswell, D.A., 1990. Petrogenesis of Mg–Cr garnet peridotites in European metamorphic belts. In: Carswell, D.A. (Ed.), Eclogite Facies Rocks. Blackie, Glasgow, pp. 260–291.

Meng, F.C., Zhang, J.X., Yang, J.S., Xu, Z.Q., 2003. Geochemical characteristics of eclogites in Xitieshan area, North Qaidam of northwestern China. Acta Petrologica Sinica 19, 435–442.

Niu, Y., 1997. Mantle melting and melt extraction processes beneath ocean ridges: evidence from abyssal peridotites. Journal of Petrology 38, 1047–1074.

Niu, Y., 1999. Comments on some misconceptions in igneous and experimental petrology and methodology: a reply. Journal of Petrology 40, 1195–1203.

Niu, Y., 2005. Generation and evolution of basaltic magmas: some basic concepts and a hypothesis for the origin of the Mesozoic–Cenozoic volcanism in eastern China. Geological Journal of China Universities 11, 9–46.

Niu, Y., Gilmore, T., Mackie, S., Greig, A., Bach, W., 2002. Mineral chemistry, whole-rock compositions and petrogenesis of ODP Leg 176 gabbros: data and discussion. In: Proceedings of the ODP, Science Results, vol. 176, 60pp.

O'Brien, P.J., 2001. Subduction followed by collision: Alpine and Himalayan examples. Physics of the Earth and Planetary Interiors 127, 277–291.

O'Hara, M.J., Mercy, E.L.P., 1963. Petrology and petrogenesis of some garnetiferous peridotites. Transactions of the Royal Society of Edinburgh 65, 251–314.

O'Neill, H.St.C., Wood, B.J., 1979. An experimental study of Fe–Mg partitioning between garnet and olivine and its calibration as a geothermometer. Contributions to Mineralogy and Petrology 70, 59–70.

Song, S.G., 1996. Metamorphic Geology of Blueschists, Eclogites and Ophiolites in the North Qilian Mountains. 30th IGC Field Trip Guide T392, Geological Publishing House, Beijing, 40pp.

Song, S.G., Yang, J.S., Xu, Z.Q., Liou, J.G., Wu, C.L., Shi, R.D., 2003a. Metamorphic evolution of coesite-bearing UHP terrane in the North Qaidam, northern Tibet, NW China. Journal of Metamorphic Geology 21, 631–644.

Song, S.G., Yang, J.S., Liou, J.G., Wu, C.L., Shi, R.D., Xu, Z.Q., 2003b. Petrology, geochemistry and isotopic ages of eclogites in the Dulan UHPM terrane, the North Qaidam, NW China. Lithos 70, 195–211.

Song, S.G., Zhang, L.F., Niu, Y., 2004. Ultra-deep origin of garnet peridotite from the North Qaidam ultrahigh-pressure belt, Northern Tibetan Plateau, NW China. American Mineralogist 89, 1330–1336.

Song, S.G., Zhang, L.F., Chen, J., Liou, J.G., Niu, Y., 2005a. Sodic amphibole exsolutions in garnet from garnet-peridotite, North Qaidam UHPM belt, NW China: implications for ultradeep-origin and hydroxyl defects in mantle garnets. American Mineralogist 90, 814–820.

Song, S.G., Zhang, L.F., Niu, Y., Su, L., Jian, P., Liu, D.Y., 2005b. Geochronology of diamond-bearing zircons from garnet peridotite in the North Qaidam UHPM belt, Northern Tibetan Plateau: a record of complex histories from oceanic lithosphere subduction to continental collision. Earth and Planetary Science Letters 234, 99–118.

Song, S.G., Zhang, L.F., Niu, Y., Su, L., Song, B., Liu, D.Y., 2006. Evolution from oceanic subduction to continental collision: a case study of the Northern Tibetan Plateau inferred from geochemical and geochronological data. Journal of Petrology 47, 435–455.

Song, S.G., Su, L., Niu, Y., Zhang, L.F., 2007a. Petrological and geochemical constraints on the origin of garnet peridotite in the North Qaidam ultrahigh-pressure Metamorphic Belt, Northwestern China. Lithos 96, 243–265.

Song, S.G., Zhang, L.F., Niu, Y., Wei, C.J., Liou, J.G., Shu, G.M., 2007b. Eclogite and carpholite-bearing meta-pelite in the North Qilian suture zone, NW China: implications for Paleozoic cold oceanic subduction and water transport into mantle. Journal of Metamorphic Geology 25, 547–563.

Spengler, D., van Roermund, H.L.M., Drury, M.R., Ottolini, L., Mason, P.R.D., Davies, G.R., 2006. Deep origin and hot melting of an Archaean orogenic peridotite massif in Norway. Nature 440, 913–917.

Streckeisen, A., 1976. To each plutonic rock its proper name. Earth Science Review 12, 1–33.

van Roermund, H.L.M., Drury, M.R., 1998. Ultra-high pressure (P > 6 GPa) garnet peridotites in Western Norway: exhumation of mantle rocks from > 185 km depth. Terra Nova, 10, 295–301.

van Roermund, H.L.M., Drury, M.R., Barnhoorn, A., de Ronde, A., 2001. Non-silicate inclusions in garnet from an ultra-deep orogenic peridotite. Geological Journal 35, 209–229.

Wu, H.Q., Feng, Y.M., Song, S.G., 1993. Metamorphism and deformation of blueschist belts and their tectonic implications, North Qilian Mountains, China. Journal of Metamorphic Geology 11, 523–536.

Yang, J.J., Powell, R., 2008. Ultrahigh-pressure garnet peridotites from the devolatilization of sea-floor hydrated ultramafic rocks. Journal of Metamorphic Geology 26, 695–716.

Yang, J.J., Godard, G., Kienast, J.R., Lu, Y., Sun, J., 1993. Ultrahigh-pressure (60 kbar) magnesite-bearing garnet peridotites from northeastern Jiangsu, China. Journal of Geology 101, 541–554.

Yang, J.J., Zhu, H., Deng, J.F., Zhou, T.Z., Lai, S.C., 1994. Discovery of garnet-peridotite at the northern margin of the Qaidam Basin and its significance. Acta Petrologica et Mineralogica 13, 97–105 (in Chinese with English abstract).

Yang, J.S., Xu, Z.Q., Song, S.G., Zhang, J., Wu, C., Shi, R., Li, H., Brunel, M., 2001. Discovery of coesite in the North Qaidam Early Palaeozoic ultrahigh pressure (UHP) metamorphic belt, NW China. Comptes Rendus De L Academie Des Sciences Serie II Fascicule A – Sciences De La Terre et Des Planetes 333 (11), 719–724.

Yang, J.S., Xu, Z.Q., Song, S.G., Zhang, J.X., Wu, C.L., Shi, R.D., Li, H.B., Brunel, M., Tapponnier, P., 2002. Subduction of continental crust in the early Paleozoic North Qaidam ultrahigh-pressure metamorphism belt, NW China: evidence from the discovery of coesite in the belt. Acta Geologica Sinica 76, 63–68.

Yang, J.S., Wu, C.L., Zhang, J.X., Shi, R.D., Meng, F.C., Wooden, J., Yang, H.Y., 2006. Protolith of eclogites in the north Qaidam and Altun UHP terrane, NW China: earlier oceanic crust? Journal of Asian Earth Sciences 28, 185–204.

Zhang, R.Y., Liou, J.G., Cong, B.L., 1994. Petrogenesis of garnet-bearing ultramafic rocks and associated eclogites in the Su–Lu ultrahigh-pressure metamorphic terrane, China. Journal of Metamorphic Geology 12, 169–186.

Zhang, R.Y., Liou, J.G., Yang, J.S., Yui, T-F., 2000. Petrochemical constraints for dual origin of garnet peridotites from the Dabie-Sulu UHP terrane, eastern-central China. Journal of Metamorphic Geololy 18, 149–166.

Zhang, G.B., Song, S.G., Zhang, L.F., Niu, Y., Shu, G.M., 2005. Ophiolite-type mantle peridotite from Shaliuhe, North Qaidam UHPM belt, NW China and its tectonic implications. Acta Petrologica Sinica 21, 1049–1058.

Zhang, J.X., Yang, J.S., Meng, F.C., Wan, Y.S., Li, H.M., Wu, C.L., 2006. U–Pb isotopic studies of eclogites and their host gneisses in the Xitieshan area of the North Qaidam mountains, western China: new evidence for an early Paleozoic HP–UHP metamorphic belt. Journal of Asian Earth Sciences 28, 143–150.

Zhang, J.X., Meng, F.C., Wan, Y.S., 2007. A cold Early Palaeozoic subduction zone in the North Qilian Mountains, NW China: petrological and U–Pb geochronological constraints. Journal of Metamorphic Geology 25, 285–304.

Zhang, G.B., Song, S.G., Zhang, L.F., Niu, Y., 2008. The subducted oceanic crust within continental-type UHP metamorphic belt in the North Qaidam, NW China: evidence from petrology, geochemistry and geochronology. Lithos 104, 99–108.